articles

molecular pharmaceutics

Targeting Nanosystems to Human DCs via Fc Receptor as an Effective Strategy to Deliver Antigen for Immunotherapy

Luis J. Cruz,*[,†,‡] Felix Rueda,[†,§] Begoña Cordobilla,[§] Lorena Simón,[‡,∥] Leticia Hosta,[‡,∥] Fernando Albericio,[‡,∥,⊥] and Joan Carles Domingo*[,§]

CIBER-BBN, Networking Centre on Bioengineering, Biomaterials and Nanomedicine, Barcelona Science Park, Josep Samitier 1, 08028 Barcelona, Spain, Department of Biochemistry and Molecular Biology, University of Barcelona, Barcelona, Spain, Institute for Research in Biomedicine, Barcelona Science Park, Josep Samitier 10, 08028 Barcelona, Spain, and Department of Chemistry, University of Barcelona, Marti i Franques 1-11, 08028 Barcelona, Spain

Received November 15, 2009; Revised Manuscript Received November 21, 2010; Accepted November 29, 2010

Abstract: Dendritic cells (DCs) are increasingly being explored as cellular vaccines for tumor immunotherapy, since they provide an effective system of antigen presentation both in vitro and in vivo. An additional advantage of this cell type is that it is possible to target specific antigens through the activation of receptors, such as FcR (the receptor for the IgG Fc fragment) and TLR (toll-like Receptor). Thus, the uptake capacity of DCs can be improved, thereby increasing antigen presentation. This, in turn, would lead to an enhanced immune response, and, in some instances, the tolerance/anergy of immune effector cells present in cancer patients could be reverted. Here we studied various nanotargeting systems, including liposomes and gold nanoparticles of a peptide-based immunotherapeutic vaccine for the treatment of androgen-responsive prostate cancer. Building blocks of the immunogenic peptide consisted of the luteinizing hormone-releasing hormone (LHRH), also known as gonadotropin-releasing hormone (GnRH) peptide (B- and T-cell epitope), in tandem with a T-helper epitope corresponding to the 830−844 region of tetanus toxoid. Three new peptides with several modifications at the N-terminal (palmitoyl, acetyl, and FITC) were synthesized. These peptides also contained a Cys as C-terminal residue to facilitate grafting onto gold nanoparticles. To target different antigen formulations to human DCs, the Fc was activated with a cross-linking spacer to generate a free thiol group and thus facilitate conjugation onto gold nanoparticles, liposomes, and peptide. Our results show that gold nanoparticles and liposomes targeted to FcRs of human DCs are effective antigen delivery carriers and induce a strong immune response with respect to nontargeted LHRH-TT-nanoparticle conjugates and a superior response to that of naked antigens. In addition, dual labeling using gold and FITC-peptide allowed DC tracking by flow cytometry as well as transmission electron microscopy. Nanoparticles were observed to show a homogeneous distribution throughout the cytoplasm. These results open up a new approach to the development of a novel strategy for cancer vaccines.

Keywords: Peptides; gold nanoparticles; dendritic cells; targeting; peptide vaccines; immunotherapeutic vaccines; cancer vaccine

1. Introduction

Vaccination against infective pathogens is one of the milestones of modern medicine and has changed the history of mankind. The specificity, strength, and persistence of the immune response have led many research teams to focus their efforts on producing vaccines against cancer. The

* To whom correspondence should be addressed. (L.J.C.) Present address: Department of Tumor Immunology, NCMLS 278, Radboud University Nijmegen Medical Centre, Geert Grooteplein 26/28, 6525 GA Nijmegen, The Netherlands. Fax: +31-24-3540339. Telephone: +31-24-3617422. E-mail: ljcruz@ncmls.ru.nl, jcruz@pcb.ub.es. (J.C.D.) Mailing address: Departament de Bioquímica i Biologia Molecular, Facultat de Biologia, Edifici Nou, Planta-1, C/Diagonal 645, 08028 Barcelona, Spain. Telephone: 93-4021214. Fax: 93-4021219. E-mail: jcdomingo@ub.edu.

† These authors contributed equally to the work.

‡ CIBER-BBN, Networking Centre on Bioengineering, Biomaterials and Nanomedicine, Barcelona Science Park.

§ Department of Biochemistry and Molecular Biology, University of Barcelona.

∥ Institute for Research in Biomedicine, Barcelona Science Park.

⊥ Department of Chemistry, University of Barcelona.

10.1021/mp100178k
Published on Web 12/01/2010

primary goal of vaccination is the generation of robust and specific cellular and humoral immune responses.[1−3] In this regard, dendritic cells (DCs) are the most efficient type of specialized antigen-presenting cells (APCs). These cells have an exceptional capacity to initiate both primary and secondary immune responses in vivo, and under the appropriate stimuli they initiate and direct antitumor immune responses.[4−6] To exert this action, DCs take up the antigen, together with danger/maturation signals which induce their activation and maturation, in a process that unleashes many essential properties required to activate the antitumor immune response.

In a natural environment, the danger/activation signals are produced by inflammatory cytokines, pathogens, or products derived from them; however, in a vaccine, these signals are made by natural or synthetic adjuvants.[7,8] Moreover, bioconjugation strategies can be used to attach molecular danger signals to particles to amplify the immune response while providing a potential nontoxic alternative adjuvant technology. Particulate delivery systems, such as ISCOMs (immunostimulatory complexes),[9,10] metallic nanoparticles (NPs),[11,12] liposomes,[13] polymers,[14] exosomes,[15] virosomes,[16] and bioconjugates,[17] present many of the mentioned characteristics.

Gold nanoparticles (AuNPs) are inert,[18] are relatively easy to prepare, and bind efficiently to a wide range of biomolecules such as DNA[19] and proteins.[20] NPs are considered to be efficient antigen (Ag) carriers and are widely studied for their biological potential.[21,22] In addition, polymer microparticles, NPs, and liposomes can protect Ag from degradation and deliver it specifically to DCs, and novel chemical strategies can be used to release Ag intracellularly so that it can be processed by both MHC class I and class II pathways. Polymers can also be used as synthetic adjuvants to induce DC maturation and initiate adaptive immune responses through various mechanisms.

One effective strategy in immunotherapy is based on loading DCs with Ag-IgG immune complexes (ICs), which leads to efficient Ag uptake, maturation of DCs, and increased MHC class I and class II restricted Ag presentation in vitro,[23−29] and T-cell priming in vivo.[27,30−32] These processes are FcγR-mediated (the receptor gamma for IgG Fc fragment). Incubation of DCs with ICs activates a "license

(1) Hutchings, C. L.; Gilbert, S. C.; Hill, A. V.; Moore, A. C. Novel protein and poxvirus-based vaccine combinations for simultaneous induction of humoral and cell-mediated immunity. *J. Immunol.* **2005**, *175*, 599–606.

(2) Paschen, A.; Eichmuller, S.; Schadendorf, D. Identification of tumor antigens and T-cell epitopes, and its clinical application. *Cancer Immunol. Immunother.* **2004**, *53*, 196–203.

(3) Spagnoli, G. C.; Adamina, M.; Bolli, M.; Weber, W. P.; Zajac, P.; Marti, W.; Oertli, D.; Heberer, M.; Harder, F. Active antigen-specific immunotherapy of melanoma: from basic science to clinical investigation. *World J. Surg.* **2005**, *29*, 692–699.

(4) Banchereau, J.; Briere, F.; Caux, C.; Davoust, J.; Lebecque, S.; Liu, Y. J.; Pulendran, B.; Palucka, K. Immunobiology of dendritic cells. *Annu. Rev. Immunol.* **2000**, *18*, 767–811.

(5) Celluzzi, C. M.; Mayordomo, J. I.; Storkus, W. J.; Lotze, M. T.; Falo, L. D., Jr. Peptide-pulsed dendritic cells induce antigen-specific CTL-mediated protective tumor immunity. *J. Exp. Med.* **1996**, *183*, 283–287.

(6) Steinman, R. M. The dendritic cell system and its role in immunogenicity. *Annu. Rev. Immunol.* **1991**, *9*, 271–296.

(7) Aucouturier, J.; Dupuis, L.; Deville, S.; Ascarateil, S.; Ganne, V. Montanide ISA 720 and 51: a new generation of water in oil emulsions as adjuvants for human vaccines. *Expert Rev. Vaccines* **2002**, *1*, 111–118.

(8) Guy, B. The perfect mix: recent progress in adjuvant research. *Nat. Rev. Microbiol.* **2007**, *5*, 505–517.

(9) Sanders, M. T.; Brown, L. E.; Deliyannis, G.; Pearse, M. J. ISCOM-based vaccines: the second decade. *Immunol. Cell Biol.* **2005**, *83*, 119–128.

(10) Skene, C. D.; Sutton, P. Saponin-adjuvanted particulate vaccines for clinical use. *Methods* **2006**, *40*, 53–59.

(11) Hosta, L.; Pla-Roca, M.; Arbiol, J.; Lopez-Iglesias, C.; Samitier, J.; Cruz, L. J.; Kogan, M. J.; Albericio, F. Conjugation of Kahalalide F with gold nanoparticles to enhance in vitro antitumoral activity. *Bioconjugate Chem.* **2009**, *20*, 138–146.

(12) Kogan, M. J.; Olmedo, I.; Hosta, L.; Guerrero, A. R.; Cruz, L. J.; Albericio, F. Peptides and metallic nanoparticles for biomedical applications. *Nanomedicine* **2007**, *2*, 287–306.

(13) Kersten, G. F.; Crommelin, D. J. Liposomes and ISCOMs. *Vaccine* **2003**, *21*, 915–920.

(14) Cruz, L. J.; Iglesias, E.; Aguilar, J. C.; Cabrales, A.; Reyes, O.; Andreu, D. Different immune response of mice immunized with conjugates containing multiple copies of either consensus or mixotope versions of the V3 loop peptide from human immunodeficiency virus type 1. *Bioconjugate Chem.* **2004**, *15*, 1110–1117.

(15) Taieb, J.; Chaput, N.; Zitvogel, L. Dendritic cell-derived exosomes as cell-free peptide-based vaccines. *Crit. Rev. Immunol.* **2005**, *25*, 215–223.

(16) Westerfeld, N.; Zurbriggen, R. Peptides delivered by immunostimulating reconstituted influenza virosomes. *J. Pept. Sci.* **2005**, *11*, 707–712.

(17) Cruz, L. J.; Iglesias, E.; Aguilar, J. C.; Gonzalez, L. J.; Reyes, O.; Albericio, F.; Andreu, D. A comparative study of different presentation strategies for an HIV peptide immunogen. *Bioconjugate Chem.* **2004**, *15*, 112–120.

(18) Merchant, B. Gold, the noble metal and the paradoxes of its toxicology. *Biologicals* **1998**, *26*, 49–59.

(19) Alivisatos, A. P.; Johnsson, K. P.; Peng, X.; Wilson, T. E.; Loweth, C. J.; Bruchez, M. P., Jr.; Schultz, P. G. Organization of 'nanocrystal molecules' using DNA. *Nature* **1996**, *382*, 609–611.

(20) Gole, A.; Dash, C.; Soman, C.; Sainkar, S. R.; Rao, M.; Sastry, M. On the preparation, characterization, and enzymatic activity of fungal protease-gold colloid bioconjugates. *Bioconjugate Chem.* **2001**, *12*, 684–690.

(21) Coester, C.; Nayyar, P.; Samuel, J. In vitro uptake of gelatin nanoparticles by murine dendritic cells and their intracellular localisation. *Eur. J. Pharm. Biopharm.* **2006**, *62*, 306–314.

(22) Dinauer, N.; Balthasar, S.; Weber, C.; Kreuter, J.; Langer, K.; von Briesen, H. Selective targeting of antibody-conjugated nanoparticles to leukemic cells and primary T-lymphocytes. *Biomaterials* **2005**, *26*, 5898–5906.

(23) Amigorena, S.; Bonnerot, C. Fc receptors for IgG and antigen presentation on MHC class I and class II molecules. *Semin. Immunol.* **1999**, *11*, 385–390.

(24) Antoniou, A. N.; Watts, C. Antibody modulation of antigen presentation: positive and negative effects on presentation of the tetanus toxin antigen via the murine B cell isoform of FcgammaRII. *Eur. J. Immunol.* **2002**, *32*, 530–540.

to kill" signal[33−35] and enables DCs to directly prime specific CD4+ (helper) and CD8+ CTL (cytotoxic T lymphocytes) responses in vivo[27] and to induce antibody responses.[36]

Mice deficient for the FcR-associated chain (required for surface expression and signaling of the activating FcγRs (FcγRI and FcγRIII)) exhibit impaired induction of DC maturation by ICs and promotion of MHC class I and class II restricted presentation. This observation thus indicates that FcγRs are required for the functions of ICs in DCs.[26]

Here we describe the design of a formulation for the potential development of a treatment for prostate cancer based on a synthetic peptide vaccine that affects hormone-deprivation therapy. The active components of the vaccine are a mixture of entirely synthetic peptide Ag that direct an immune response against LHRH. The first immunological approaches for the development of LHRH vaccines date from the nineties. These were designed and tested in men to achieve androgen deprivation as a treatment of prostate cancer and in postmenopausal women to test the capacity to inhibit gonadotropins.[37−39] The efficacy of neutralizing LHRH/GnRH action through the involvement of hormone-specific antibodies has been demonstrated in a wide range of animal species, including humans.[40] Furthermore, passive immunization by infusion of anti-LHRH antibodies[41] and active vaccination with synthetic LHRH peptides coupled to tetanus or diphtheria toxoid (DT) molecules as carriers[37−39,42,43] and to multiple antigen peptide (MAP) constructs have been carried out.[44]

Our strategy was to induce an "anti-self" immunity to LHRH by altering the target molecule on a synthetic peptide immunogen. Immunization in vitro with LHRH peptide immunogens produced the desired T-cell proliferation. We developed entirely synthetic LHRH-TT (tetanus toxoid fragment) immunogens linked to AuNPs or encapasulated in liposomes. These two carrier systems have advantages and disadvantages. To reduce the undesirable effects of drugs, a primary goal for delivery systems is to use less frequent administration to achieve a constant therapeutic concentration of drug in the systemic circulation or at the specific target organ site. Among the strategies for drug delivery, colloidal carriers are effective. The most popular and well-studied colloidal drug delivery systems are liposomes. These allow high drug load and are relatively easy to handle. However, they have some fundamental problems, such as susceptibility to degradation by lysosomes and noncontrollable drug release

(25) Berg, M.; Uellner, R.; Langhorne, J. Fc gamma receptor II dependency of enhanced presentation of major histocompatibility complex class II peptides by a B cell lymphoma. *Eur. J. Immunol.* **1997**, *27*, 1022–1028.
(26) Regnault, A.; Lankar, D.; Lacabanne, V.; Rodriguez, A.; Thery, C.; Rescigno, M.; Saito, T.; Verbeek, S.; Bonnerot, C.; Ricciardi-Castagnoli, P.; Amigorena, S. Fcgamma receptor-mediated induction of dendritic cell maturation and major histocompatibility complex class I-restricted antigen presentation after immune complex internalization. *J. Exp. Med.* **1999**, *189*, 371–380.
(27) Schuurhuis, D. H.; Ioan-Facsinay, A.; Nagelkerken, B.; van Schip, J. J.; Sedlik, C.; Melief, C. J.; Verbeek, J. S.; Ossendorp, F. Antigen-antibody immune complexes empower dendritic cells to efficiently prime specific CD8+ CTL responses in vivo. *J. Immunol.* **2002**, *168*, 2240–2246.
(28) Serre, K.; Machy, P.; Grivel, J. C.; Jolly, G.; Brun, N.; Barbet, J.; Leserman, L. Efficient presentation of multivalent antigens targeted to various cell surface molecules of dendritic cells and surface Ig of antigen-specific B cells. *J. Immunol.* **1998**, *161*, 6059–6067.
(29) Swanson, J. A.; Hoppe, A. D. The coordination of signaling during Fc receptor-mediated phagocytosis. *J. Leukocyte Biol.* **2004**, *76*, 1093–1103.
(30) Akiyama, K.; Ebihara, S.; Yada, A.; Matsumura, K.; Aiba, S.; Nukiwa, T.; Takai, T. Targeting apoptotic tumor cells to Fc gamma R provides efficient and versatile vaccination against tumors by dendritic cells. *J. Immunol.* **2003**, *170*, 1641–1648.
(31) Kalergis, A. M.; Ravetch, J. V. Inducing tumor immunity through the selective engagement of activating Fcgamma receptors on dendritic cells. *J. Exp. Med.* **2002**, *195*, 1653–1659.
(32) Rafiq, K.; Bergtold, A.; Clynes, R. Immune complex-mediated antigen presentation induces tumor immunity. *J. Clin. Invest.* **2002**, *110*, 71–79.
(33) Bennett, S. R.; Carbone, F. R.; Karamalis, F.; Flavell, R. A.; Miller, J. F.; Heath, W. R. Help for cytotoxic-T-cell responses is mediated by CD40 signalling. *Nature* **1998**, *393*, 478–480.
(34) Ridge, J. P.; Di Rosa, F.; Matzinger, P. A conditioned dendritic cell can be a temporal bridge between a CD4+ T-helper and a T-killer cell. *Nature* **1998**, *393*, 474–478.
(35) Schoenberger, S. P.; van der Voort, E. I.; Krietemeijer, G. M.; Offringa, R.; Melief, C. J.; Toes, R. E. Cross-priming of CTL responses in vivo does not require antigenic peptides in the endoplasmic reticulum of immunizing cells. *J. Immunol.* **1998**, *161*, 3808–3812.
(36) Getahun, A.; Dahlstrom, J.; Wernersson, S.; Heyman, B. IgG2a-mediated enhancement of antibody and T cell responses and its relation to inhibitory and activating Fc gamma receptors. *J. Immunol.* **2004**, *172*, 5269–5276.
(37) Gual, C.; Garza-Flores, J.; Menjivar, M.; Gutierrez-Najar, A.; Pal, R.; Talwar, G. P. Ability of an anti-luteinizing hormone-releasing hormone vaccine to inhibit gonadotropins in postmenopausal women. *Fertil. Steril.* **1997**, *67*, 404–407.
(38) Simms, M. S.; Scholfield, D. P.; Jacobs, E.; Michaeli, D.; Broome, P.; Humphreys, J. E.; Bishop, M. C. Anti-GnRH antibodies can induce castrate levels of testosterone in patients with advanced prostate cancer. *Br. J. Cancer* **2000**, *83*, 443–446.
(39) Talwar, G. P. Vaccines for control of fertility and hormone-dependent cancers. *Immunol. Cell Biol.* **1997**, *75*, 184–189.
(40) Naz, R. K.; Rajesh, C. Passive immunization for immunocontraception: lessons learned from infectious diseases. *Front. Biosci.* **2004**, *9*, 2457–2465.
(41) Silversides, D. W.; Murphy, B. D.; Misra, V.; Mapletoft, R. J. Monoclonal antibodies against LHRH: development and immunoactivity in vivo and in vitro. *J. Reprod. Immunol.* **1985**, *7*, 171–184.
(42) Finstad, C. L.; Wang, C. Y.; Kowalski, J.; Zhang, M.; Li, M. L.; Li, X. M.; Xia, W. G.; Bosland, M. C.; Murthy, K. K.; Walfield, A. M.; Koff, W. C.; Zamb, T. J. Synthetic luteinizing hormone releasing hormone (LHRH) vaccine for effective androgen deprivation and its application to prostate cancer immunotherapy. *Vaccine* **2004**, *22*, 1300–1313.
(43) Talwar, G. P. Fertility regulating and immunotherapeutic vaccines reaching human trials stage. *Hum. Reprod. Update* **1997**, *3*, 301–310.
(44) Beekman, N. J.; Schaaper, W. M.; Turkstra, J. A.; Meloen, R. H. Highly immunogenic and fully synthetic peptide-carrier constructs targetting GnRH. *Vaccine* **1999**, *17*, 2043–2050.

rate. NPs, in general, can be used to improve oral bioavailability, to sustain effect in target tissue, and to improve the stability of therapeutic agents against enzymatic or lysosomal degradation. NPs are solid, porous spheres, and the drug is attached by sorptive processes. In liposomes, the drugs are mostly encapsulated or strongly associated with the lipid bilayer. The body distribution of both carrier systems is influenced mainly by particle size and surface properties such as charge and hydrophilicity. In addition, we included the Fc fragment of human IgG as a targeting system in the same NPs and liposomes. These Ag, which are bound to these delivery systems and conjugated with fluorescein, have shown their utility for the study of APC Ag uptake by flow cytometry, confocal microscopy, and transmission electron microscopy. At the same time, we report on the efficiency of several nanoformulations as Ag carriers. In this regard, the nanoformulations (AuNP and liposomes) showed superior performance to that of the peptide alone for intracellular uptake and Ag presentation. Finally, we demonstrate the advantages of targeting nanoformulations to specific receptors in DCs, such as to FcγR.

2. Material and Methods

2.1. Materials and Reagents. Fmoc-Nα-protected amino acids were purchased from IRIS Biotech GmbH (Marktredwitz, Germany). The ChemMatrix resin was obtained from Matrix Innovation, Canada. Coupling reagents are as follows: PyAOP was obtained from Applied Biosystems (Foster City, CA), PyBOP from Novabiochem (Laüfelfingen, Switzerland), HOAt from GL Biochem (Shanghai, China), and TBTU from Matrix Innovation. DIEA, DIPCDI, piperidine, TFA, and MeCN (HPLC grade) were from Merck (Darmstadt, Germany), Scharlau (Barcelona, Spain), and Panreac (Barcelona, Spain). DMF, DCM, and methanol were obtained from SDS (Peypin, France). 5(6)-Carboxyfluorescein was from Acros (Somerville, NJ). Triisopropylsilane (TIS) was purchased from Fluka (Buchs, Switzerland). The other chemicals used were obtained from Aldrich (Milwaukee, WI) and were of the highest purity commercially available. Egg phosphatidylcholine (PC), phosphatidylglycerol (PG) from egg yolk lecithin, *N*-succinimidyl-3-(2-pyridyldithio)-propionate (SPDP), sulfosuccinimidyl-4-(*N*-maleimidomethyl) cyclohexane-1-carboxylate (SMCC), and dithiothreitol (DTT) were obtained from Sigma Chemical Co. (St. Louis, MO), and 1,2-distearoyl-*sn*-glycero-3-phosphoethanolamine-*N*-[maleimide(polyethylene glycol)-3400] (ammonium salt) (DSPE-PEG-Mal) was from Shearwater Polymers (Birmingham, AL).

Peptides were analyzed by high pressure liquid chromatography (HPLC) on Symmetry C18 columns (4.6 × 150 mm, 5 μm) (Waters, Ireland), using a linear gradient of 0−100% of CH_3CN (+0.036% TFA) to H_2O (+0.045% TFA) run over 15 min at a flow rate of 1.0 mL/min. Detection was at 220 nm on a Waters instrument 996 photodiode array detector equipped with a Waters 2695 separation module and Millennium software. Mass spectra were recorded on a MALDI Voyager DE RP time-of-flight (TOF) spectrometer (PE Biosystems, Foster City, CA).

2.2. Peptide Synthesis and Characterization. The peptides *X*-LHRH-Ala-Ala-TTβAlaCys (EHWSYGLRPGAAQY-IKANSKFIGITELKK-βAlaCys-NH_2) (*X* = acetic acid, palmitic acid, and 5(6)-carboxyfluorescein) were synthesized manually following standard protocols of solid-phase peptide synthesis using a Fmoc/*tert*-butyl (*t*-Bu) strategy on aminomethyl ChemMatrix resin (0.1 mmol, 0.4 mmol/g).[45] The linker was coupled manually using Fmoc-Rink linker (3 equiv), PyBOP (3 equiv), HOAt (3 equiv), and DIEA (9 equiv) in DMF. Before Fmoc removal, an acetylating step was performed to block possible free amino groups. Side-chain-protecting groups were *tert*-butyl for Glu, Thr, Ser, and Tyr; trityl for Gln and Asn; Boc for Lys; and 2,2,5,7,8-pentamethylchroman-6-sulfonyl for Arg. Nα-Fmoc-protected amino acids were incorporated using HOBt and DIPCDI in DMF for 1.5 h and monitored by Kaiser ninhydrin tests.[46] When required, recouplings were performed with TBTU, HOBt, and DIEA in DMF. The Fmoc-protecting group was cleaved with a 20% piperidine solution in DMF (2 × 10 min). After completion of the sequence, the peptide-resin was split in three similar parts. For the first part, the LHRH-TT peptide resin was acetylated (Ac) with [Ac_2O/DIEA/DMF (10/5/85)] for 1 h. For the second part, palmitoyl acid (4 equiv) dissolved in DMF was coupled to PyBOP (4 equiv) and DIEA (8 equiv) overnight, while for the third part the peptide resin was labeled with 5(6)-carboxyfluorescein (CF). CF (5 equiv), PyAOP (5 equiv), HOAt (5 equiv), and DIEA (10 equiv) were preactivated with DMF/DCM (9/1) for 10 min and then added to the peptide resin and stirred for 12 h.

All the peptides were cleaved from the resin by treatment with 95% TFA, 2.5% TIS, and 2.5% water for 2 h. All peptides were characterized by analytical reverse phase (RP)-HPLC (tR) and MALDI-TOF.

The FITC-LHRH-TT peptide was cleaved using TFA/TIS/H_2O (95/2.5/2.5) for 90 min. The peptide was characterized by analytical RP-HPLC (tR 6.8 min, 43%) and MALDI-TOF (*m*/*z* calcd, 3822.51; found, 3823. 45 $[M + H]^+$).

The pamitoyl-LHRH-TT peptide was cleaved using TFA/TIS/H_2O (95/2.5/2.5) for 90 min. The peptide was characterized by analytical RP-HPLC (tR 7.9 min, 54%) and MALDI-TOF (*m*/*z* calcd, 3702.39; found, 3703.87 $[M + H]^+$).

The Ac-LHRH-TT peptide was cleaved using TFA/TIS/H_2O (95/2.5/2.5) for 90 min. The peptide was characterized by analytical RP-HPLC (tR 6.7 min, 57%) and MALDI-TOF (*m*/*z* calcd, 3520.05; found, 3521.51 $[M + H]^+$).

All the peptides were purified by dialysis (for 3 days in a membrane Spectra/MWCO: 1000) against water, and the solution was changed at least three times per day.

(45) Fields, G. B.; Noble, R. L. Solid phase peptide synthesis utilizing 9-fluorenylmethoxycarbonyl amino acids. *Int. J. Pept. Protein Res.* **1990**, *35*, 161–214.

(46) Kaiser, E.; Colescott, R. L.; Bossinger, C. D.; Cook, P. I. Color test for detection of free terminal amino groups in the solid-phase synthesis of peptides. *Anal. Biochem.* **1970**, *34*, 595–598.

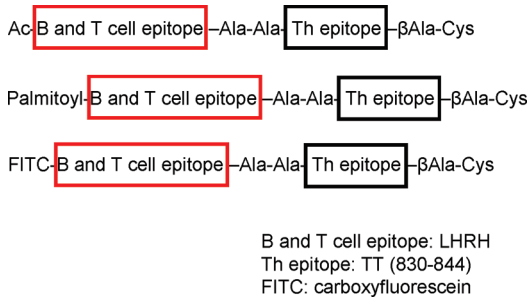

2.3. Conjugation of Peptide to the Fc Fragment. Peptides were conjugated to the Fc fragment using the heterobifunctional reagent SMCC. Briefly, the Fc fragment from human IgG (Acris Antibodies GmbH, Hiddenhausen, Germany) (1 mg/mL in PBS, 100 uL) was activated with SMCC reagent (SMCC/Fc, 15/1 molar ratio) for 1 h at 25 °C. Excess SMCC was removed by using a Sephadex G-50 spin column. The Fc fragment activated with maleimide group was added to FITC-LHRH-TT-Cys (1 mg/mL in water, 200 uL) for 3 h at 25 °C. Excess peptide was removed by using a Sephadex G-25 column. A molar ratio of 10 FITC-peptide per Fc fragment was found.

2.4. Preparation of Peptide-Conjugated AuNPs and Targeting Them with the Fc Fragment. AuNPs were produced by reduction of hydrogen tetrachloroaurate ($HAuCl_4 \cdot H_2O$) (Aldrich, Milwaukee, WI). $HAuCl_4 \cdot H_2O$ (8.7 mg) was added to a sodium citrate solution (100 mL, 2.2 mM) at 150 °C. The reducing agent was added rapidly, and the reaction was allowed to continue under uniform and vigorous stirring until the solution turned red.[47] The conjugation was made in the presence of an excess of peptide and protein.[48] Peptides (1 mg solubilized in 1 mL of water) were added dropwise to a 10 mL solution of AuNPs at room temperature with magnetic stirring, and agitation was maintained for 15 min. The AuNP complexes were then purified by dialysis (for 3 days in a membrane Spectra/MWCO: 6−8000) against sodium citrate 2.2 mM, and the solution was changed at least two times per day. To determine the number of peptide molecules per NP, nondialyzed aliquots of the conjugated solutions (2.5 mL) were centrifuged at 14 000 rpm for 10 min. The supernatant was lyophilized and then analyzed by RP-HPLC to determine the amount of unconjugated peptide. It was observed that 47 ± 2.1% (470 μg) of peptides was conjugated to the AuNPs (10 mL solution of AuNPs).

To bind Fc fragments and peptide to AuNPs, the Fc protein (2 mg/mL in PBS) was conjugated with the heterobifunctional reagent SPDP (SPDP/Fc, 15/1 molar ratio). Excess SPDP was removed by using a Sephadex G-50 spin column. As estimated spectrophotometrically, there were four PDP residues per Fc molecule. Thiolated Fc (Fc-SH) was obtained by reducing the Fc-PDP with DTT 50 mM at pH = 4.5. Excess DTT was removed by using a Sephadex G-50 spin column. The protein with reduced thiols was kept in a N_2 atmosphere and used immediately. Freshly prepared Fc-SH fragments (a molar ratio of 30 PDP/Fc AuNP and a 1 mg/mL). Therefore, the activated Fc was added dropwise to the same AuNP solution. The Au complexes were purified by centrifugation using amicon 100 kDa (Centriplus, Millipore Corporation) to remove the excess of the peptide (3.5 kDa) and Fc (around 50 kDa).

In order to determine the amount of peptide and Fc per AuNP solution, the peptide and Fc were separated by amicon 10 kDa. Thus, the Fc fraction was retained and concentrated by the filter while the peptide fraction was collected in the flow-through. The concentration of Fc protein was determined by the Coomassie dye protein assay, and the peptide fraction, after lyophilization, was measured by RP-HPLC. It was observed that 26 ± 2.1% (260 μg) of peptides and 11 ± 1.3% (110 μg) of Fc were conjugated to the AuNP solution.

2.5. Preparation of Liposomes and Peptide Encapsulation. Unilamellar liposomes were prepared as described elsewhere.[49] Briefly, a lipid mixture of EPC/PG/palmitoyl-peptide 80/20/10 molar ratio was suspended in PBS buffer and sequentially extruded through a 0.1 μm pore size polycarbonate membrane (Nucleopore) at 60 °C in an extrusion device (Liposofast, Avestin Inc.). Vesicle size was characterized by dynamic laser light scattering using a PCS41 optic unit (Malvern Autosizer IIC). The polydispersity index as an estimation of the particle size distribution width is calculated from a simple two-parameter fit to the correlation data called a cumulants analysis of the dynamic light scattering measured intensity autocorrelation function. The polydispersity index is dimensionless and scaled between 0.05−0.7. The entrapment efficiency of palmitoyl-peptide within liposomes was 75 ± 3.5%.

2.6. Preparation of Targeted Liposomes with the Fc Fragment of Human IgG Conjugated to PEG. Unilamellar liposomes were prepared as above but containing 1% of DSPE-PEG-Mal.[49] Fc fragments were bound to the liposomes as described above. Freshly prepared Fc-SH was mixed with liposomes containing the coupling lipid, DSPE-PEG-Mal (a molar ratio of 20 Mal/Fc and a 1 mg/mL of lipid concentration), and was incubated for 24 h at room temperature, with stirring. It was observed that 70.0 ± 4.1% of peptides and 19.0 ± 1.3% of the Fc were conjugated to liposomes. Vesicle size was characterized by dynamic laser light scattering using a PCS41 optic unit (Malvern Autosizer IIC).

(47) Sagara, T.; Kato, N.; Nakashima, N. Electroreflectance Study of Gold Nanoparticles Immobilized on an AminoalkanethiolMonolayer Coated on a Polycrystalline Gold Electrode Surface. *J. Phys. Chem. B* **2002**, *106*, 1205–1212.

(48) Kogan, M. J.; Bastus, N. G.; Amigo, R.; Grillo-Bosch, D.; Araya, E.; Turiel, A.; Labarta, A.; Giralt, E.; Puntes, V. F. Nanoparticle-mediated local and remote manipulation of protein aggregation. *Nano Lett.* **2006**, *6*, 110–115.

(49) Mercadal, M.; Domingo, J. C.; Petriz, J.; Garcia, J.; de Madariaga, M. A. Preparation of immunoliposomes bearing poly(ethylene glycol)-coupled monoclonal antibody linked via a cleavable disulfide bond for ex vivo applications. *Biochim. Biophys. Acta* **2000**, *1509*, 299–310.

2.7. Cell Isolation and Generation of Human DCs. Human monocytes were purified from peripheral blood mononuclear cells (PBMCs) isolated from fresh Buffy Coats (kindly provided by the Center of Transfusion and Tissue Bank of Barcelona) using a Ficoll−Paque gradient (Amersham Bioscience, Uppsala, Sweden). The interface band containing the mononuclear cells (MNCs) was withdrawn. Cells were then washed in saline solution and centrifuged twice at 1500 rpm to remove platelets. Monocytes were obtained by 20 min plastic adherence of 20×10^6 PBMC/mL onto a gelatin-coated flask. Nonadherent cells were withdrawn and frozen (10% DMSO, 90% autologous serum) for use as autologous lymphocyte source. The adherent cells (70−80% monocytes) were detached with EDTA 10 mM for 30 min. Then they were then seeded (1×10^6 cells/well) into 6-well plates (Costar, Cambridge, MA).

A negative selection purification method using Monocyte Negative Isolation Kit II, following the manufacturer's instructions, was also used (Dynal Biotech ASA, Olso, Norway). Briefly, cells were resuspended at 5×10^7 MNC/mL in BSA 0.1%. A blocking reagent and antibody mixture was added, and cells were then incubated for 10 min at 4−8 °C. They were then washed and centrifuged for 8 min at 500*g*. Washed beads were added to cells and incubated for 15 min at 4−8 °C. Then cells were placed in a Dynal magnetic particle concentrator (MPC), and supernatant (with monocytes) was transferred to a fresh tube. After magnetic retention of the Dynabeads attached to the cells, the supernatant fraction was analyzed for the presence of the monocytic surface marker CD14. This fraction was found to contain more than 85% positive cells.

Monocytes were then differentiated to immature DCs (iDCs) by adding IL-4 (750 U/mL; Sigma Aldrich, St. Louis, MO) and GM-CSF (100 ng/mL; Leucomax 400; Novartis, Barcelona, Spain) in RPMI medium. Cultures were fed with cytokines every 2−3 days. At day 6, cells showed phenotypic characteristics of iDCs (the monocytic marker CD14 is negative; the costimulatory molecules CD80, CD86, and the immune regulator CD83 have a low expression, whereas the DC marker CD1a and the Ag of the major hystocompatibility complex HLA-DR present a high expression; these surface markers define DC populations with respect to other blood cells). When mature DCs were required, lipopolysaccaride (LPS, 500 ng/mL; Sigma Aldrich, St. Louis, MO; EC 055: B5) or TNF-α (5 ng/mL) + PGE2 (1 μM) (Sigma Aldrich, St. Louis, MO) was added at day 6 and DCs were cultured for 2 additional days (in mature DCs, CD80, CD86, and CD83 are increased).

2.8. Pulsing DCs with AuNPs, Liposomes, or Soluble Peptide. All nanoformulations and soluble peptide at a concentration of 2 and 10 μg/mL of peptide were incubated overnight with 1×10^6 DCs/mL or otherwise for the time indicated. After pulsing, DCs were washed and allowed to mature and after 3 days co-cultivated with T-cells as described below. In other processes, when maturation was not required, DCs pulsed with Ag-conjugated NPs were used at the times and in the form indicated in the corresponding section.

2.9. Flow Cytometry. Nanoformulations and peptide binding were performed by incubating human DCs with equal amounts of FITC-peptide (10 ug/mL) free and in nanoformulations for 1 h at 4 °C in culture medium. Subsequently, DCs were washed three times with PBS to remove nonspecific binding. Cells were then analyzed by flow cytometry. Intracellular uptake was performed by incubating DCs with equal amounts of FITC-peptide (10 ug/mL) free and in nanoformulations at various time points (1, 2, 4, and 24 h) at 37 °C. DCs without any FITC-labeled material, processed under the same conditions, were used as negative controls. Data for at least 1×10^5 DCs region/sample and by triplicate were acquired and analyzed on a Coulter XL flow cytometer using CellQuest and WinMDI software.

In order to determine the role of FcR in the binding and uptake of the targeted preparations, an FcR blocking reagent (MACS, Miltenyi Biotec) was used. To this end, when indicated, before performing the binding and uptake assays, we incubated samples with 50 uL for each 100 000 DCs of FcR blocking reagent (MACS, Miltenyi Biotec) for 30 min at 4 °C, after which the tests were carried out under the same conditions as described above.

2.10. Confocal Laser Scanning Microscopy (CLSM). DCs cultured on slides were incubated with various immunogens at 37 °C at a range of times to study Ag loading. The samples were fixed with paraformaldehyde and observed under confocal microscopy. CLSM was performed using an Olympus Fluoview 500 confocal microscope with a $60\times/_{1.4}$ NA (numerical aperture) objective. Fluorescence was excited with the 488 nm line of an argon laser, and its emission was detected over 515−530 nm. The microscope settings were identical for each sample and dose.

2.11. Transmission Electron Microscopy (TEM) of Bare AuNPs. Drops of bare AuNPs and liposomes were deposited over carbon-coated Formvar films on copper grids. The liposomes were stained with 2% uranyl acetate for 20 min. The samples were viewed with a transmission electron microscope (JEOL JEM 1010 (Japan)) at an accelerating voltage of 80 kV. The images were obtained with a CCD Megaview III (SIS) camera (Münster, Germany). The AuNPs measured approximately 13.1 ± 3.6 nm.

2.12. DC Cultures and AuNP Localization by TEM. DCs were fixed with 2.5% glutaraldehyde in phosphate buffer. Cells were kept in the fixative at 4 °C for 24 h. They were then washed with the same buffer and postfixed with 1% osmium tetraoxide in the same buffer containing 0.8% potassium ferricyanide at 4 °C. The samples were then dehydrated in acetone, infiltrated with Epon resin for 2 days, embedded in the same resin, and polymerized at 60 °C for 48 h. Ultrathin sections were obtained using a Leica Ultracut UCT ultramicrotome and then mounted on Formvar-coated copper grids. The sections were stained with 2% uranyl

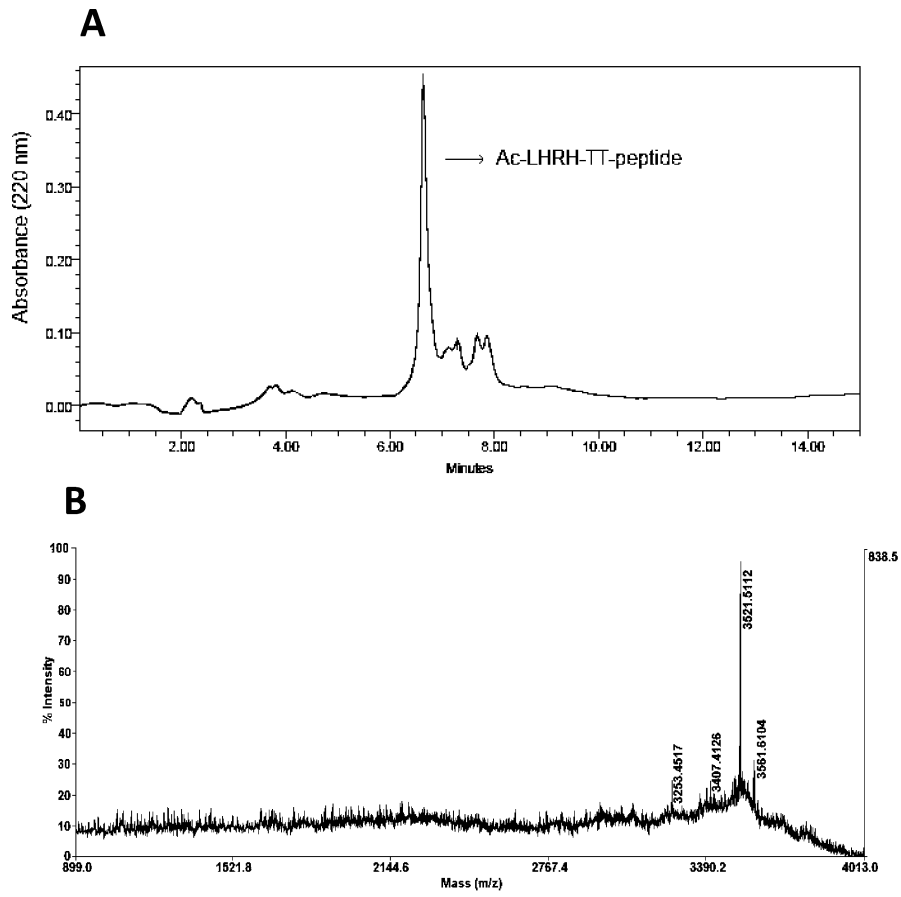

Figure 1. Representative analytical characterization of the peptides. (A) RP-HPLC analysis of Ac-LHRH-TT peptide using a linear gradient of 0−100% of CH_3CN (+0.036% TFA) to H_2O (+0.045% TFA) run over 15 min at a flow rate of 1.0 mL/min and detected at 220 nm. (B) MALDI-TOF spectrum of the main HPLC fraction (labeled with an arrow in panel A).

acetate in water and lead citrate and observed in a JEM-1010 electron microscope (Jeol, Japan).

2.13. Autologous Stimulation of Lymphocytes by DCs. Primary DCs were pulsed with Staphylococcal enterotoxin B (SEB) (Sigma, St. Louis, MO) and 1 μg/mL Ag as a positive control for 4 h at 37 °C, in a humid atmosphere of 5% CO_2. In order to block proliferation while still allowing T-cell stimulation, DCs were irradiated prior to coincubation with lymphocytes. The same process was performed by incubating DCs with the all nanoformulations and naked peptides at a concentration of 2 and 10 μg/mL of peptide, as indicated. Autologous stimulation was conducted in 96-well culture plates in RPMI 1640 containing 10% inactivated FCS and antibiotics. For each Ag, DCs were mixed with 1 $\times$ 10^5 autologous lymphocytes at a DC/lymphocyte ratio between 1/10 and 1/20 with a final volume of 200 μL. Phytohemagglutinin (PHA)-stimulated lymphocytes were used as positive controls. Cells proliferated for 72 h, and during the last 18 h 50 μL of ^{3}H-thymidine 1 mCi/mL was added to the culture. Radioactivity incorporated to DNA was measured in a beta counter in 5 mL of scintillation liquid, and the results were expressed as counts per minute (cpm).

2.14. Statistical Analysis. Statistical analyses were conducted using GraphPad Prism and Microsoft Excel software. Averages and standard deviations (SDs) were determined using standard functions. Two-way or one-way ANOVA analysis with the Dunnett's multiple comparison test was performed to determine statistical significance of the variances. The Student's *t* test was done for statistical analysis of the variance between groups.

3. Results and Discussion

3.1. Preparation and Characterization of Targeted AuNPs and Liposomes. The chimeric immunogens, containing both the target LHRH decapeptide site and a helper T-cell epitope, were prepared by a solid-phase approach. The two domains (LHRH and T epitope) were separated by two Ala residues as spacer. Two additional changes were made at both the C-terminal and the N-terminal. Thus, a Cys residue was added at the C-terminal of some LHRH-TT peptides to allow grafting onto the Au surface of NPs by covalent bonding. Three N-terminal modifications were carried out with the following: (i) carboxyfluorescein, to allow tracking by confocal microscopy and flow cytometry; (ii) acetylation, to be used in the lymphocyte proliferation assay as an experimental control; (iii) palmitoylation, to improve the encapsulation in liposomes (70.0 $\pm$ 4.1% of palmitoyl-peptide vs 27.8 $\pm$ 4.5% free peptide efficiencies).

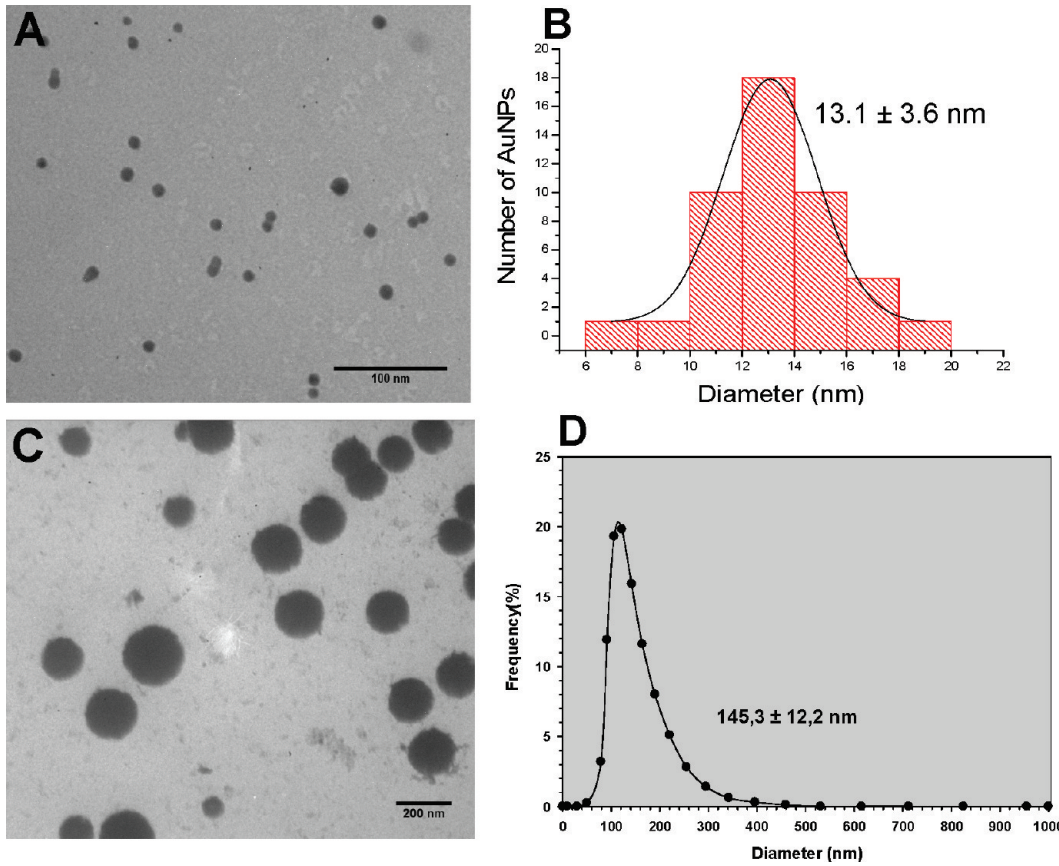

Figure 2. Characterization of AuNPs and liposomes by TEM. (A) TEM image of a representative AuNP. AuNPs were produced with sodium cytrate as the reducing agent. (B) Histogram of AuNPs. (C) TEM images of liposomes (containing palmitoyl peptide), after staining with 2% uranyl acetate; the dark color is due to the interaction between lipids from the liposomes and uranyl acetate. (D) Nanoliposomal size distribution obtained by dynamic laser light scattering. The histogram shows that the liposomes containing palmitoyl-peptide or palmitoyl-peptide-FITC had a mean diameter of around 145 ± 12 nm. The samples were viewed with a transmission electron microscope (JEOL JEM 1010, Japan) at an accelerating voltage of 80 kV. The images were obtained with a CCD Megaview III (SIS) camera (Münster, Germany).

All these modified peptides were also performed in solid-phase and the final products were characterized by RP-HPLC and mass spectroscopy (as described in Materials and Methods). Figure 1 shows a representative analytical characterization of the peptides.

In order to prepare the targeting nanosystems, the Fc (fragment of IgG protein) was activated with the heterobifunctional SPDP reagent to generate a thiol group and to facilitate conjugation to the AuNPs, liposomes, and peptides.

AuNPs were obtained via the sodium citrate reduction method,[50−53] which allows the synthesis of nanostructures of about 13 nm by adding reducing agent.[54] The AuNPs were characterized using UV−vis spectroscopy and TEM. Figure 2A and B shows the spherical morphology and a size distribution of around 13 ± 3.6 nm. UV−vis spectra of Au colloids displayed a single absorption peak in the visible range at about 525 nm (data not shown).

The liposomes were prepared by the extrusion technique through 100 nm filters. The morphology and size distribution of the liposomes was determined by TEM (Figure 2C) and dynamic light scattering (DLS; Figure 2D), respectively. The liposomes were spherical and had an average size of 145 ±

(50) Hogemann, D.; Ntziachristos, V.; Josephson, L.; Weissleder, R. High throughput magnetic resonance imaging for evaluating targeted nanoparticle probes. *Bioconjugate Chem.* **2002**, *13*, 116–121.

(51) Liu, J.; Zhang, Q.; Remsen, E. E.; Wooley, K. L. Nanostructured materials designed for cell binding and transduction. *Biomacromolecules* **2001**, *2*, 362–368.

(52) Marinakos, S. M.; Anderson, M. F.; Ryan, J.; Martin, L. D.; Feldheim, D. L. Encapsulation, Permeability, and Cellular Uptake Characteristics of Hollow Nanometer-Sized Conductive Polymer Capsules. *J. Phys. Chem. B* **2001**, *105*, 8872–8876.

(53) West, J. L.; Halas, N. J. Applications of nanotechnology to biotechnology commentary. *Curr. Opin. Biotechnol.* **2000**, *11*, 215–217.

(54) Bauer, G.; Hassmann, J.; Walter, H.; Haglmuller, J.; Mayer, C.; Schalkhammer, T. Resonant nanocluster technology: from optical coding and high quality security features to biochips. *Nanotechnology* **2003**, *14*, 1289–1311.

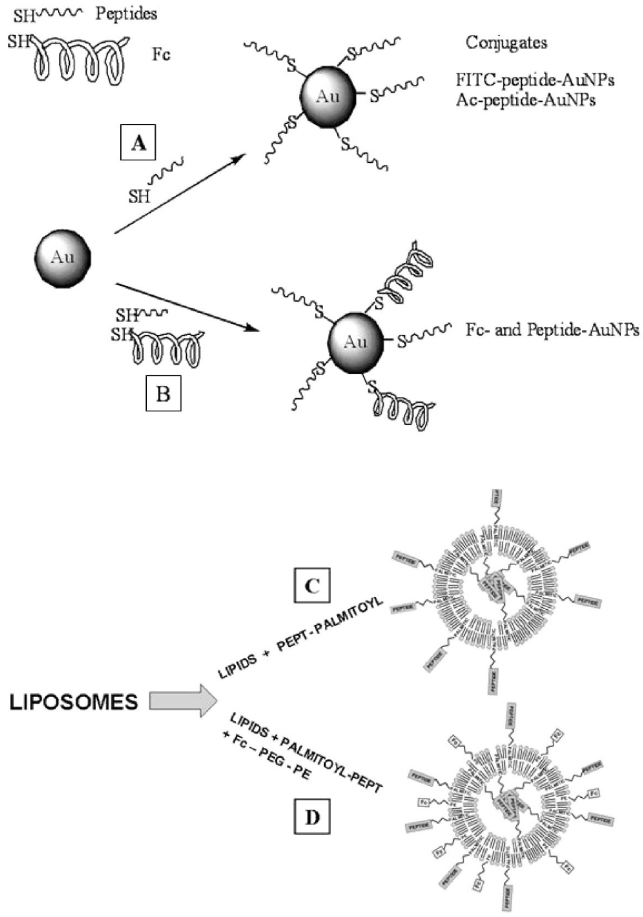

Figure 3. Schematic procedure of preparation of AuNPs and liposomes. (A) Conjugation of peptide (acetylated (Ac) or FITC labeled) to AuNPs. (B) Fc fragment was conjugated to AuNPs obtained as in (A) for targeting them to FcR. (C) Encapsulation of palmitoyl-peptide (FITC labeled or not) to liposomes. (D) Fc fragment was conjugated as in B to palmitoyl-peptide-encapsulated liposomes for targeting to FcR.

0.2 nm with a polydispersity index (P) of 0.084 ± 0.004. These observations are in accordance with previous results.[49]

The FITC-LHRH-TT-Cys and Ac-LHRH-TT-Cys peptides were conjugated separately to AuNPs as well as in combination with activated Fc (Figure 3A and B). The excess of peptide and Fc protein were removed by centrifugation using an amicon (100 kDa). To determine the degree of conjugation of the peptide and Fc protein on the NPs, we used a combination of several techniques, such as RP-HPLC and Coomassie dye protein assay for the Fc protein.

The FITC-labeled and unlabeled palmitoyl-peptides were encapsulated separately in liposomes in order to track and monitor T-cell proliferation, respectively. Liposomes targeted to the FcR were obtained by conjugation of thiol Fc fragment on the activated liposome surface with the maleimide group, as described in Material and Methods (Figure 3C and D shows a schematic representation). Also, the FITC-peptide was directly conjugated to the Fc fragment using a maleimide strategy.

3.2. Analysis of Binding and Kinetic Uptake of Distinct Nanoformulations by Flow Cytometry. Binding to DCs was analyzed at 4 °C by flow cytometry with all the constructions in which the LHRH-TT peptide was labeled with FITC. The presence of Fc strongly increased the interactions of all the constructs with respect to their counterparts without Fc (Figure 4A). The differences between them (peptide-Fc < Liposomes-Fc < AuNP-Fc) could be attributed to the increased density ratio between FITC-labeled peptide and NP; however, the initial peptide concentration added to each system was the same in each case. However, the number of FITC-labeled peptides introduced into the cells with each interaction with a specific receptor when NPs or liposomes were used was higher than that for an isolated peptide, as would be expected for an efficient delivery system.

The results of the uptake (Figure 4B) are coincident with those of the binding, thus higher binding corresponded to greater uptake. In fact, the kinetic uptake should be considered the summation of the peptides or constructs in the surface (binding) and inside the cell. As in the binding assay, the presence of Fc in the preparations increased the uptake with respect to their counterparts without Fc (Figure 4B). However, differences were not so marked, suggesting that DCs phagocytose all the preparations in those in vitro conditions (not biodistribution as in an in vivo assay); despite this, the Fc-receptor interaction was more efficient.

In order to determine the contribution of the Fc−receptor interaction to the binding and uptake process, for each condition assayed and prior to the assays, samples were treated in parallel with or without an FcR-blocking reagent and were then processed under the same conditions as described (Figure 4C and D).

Both binding and uptake were affected when Fc-targeted preparations were treated with the FcR-blocking agent; however, while the binding was abolished (Figure 4C), uptake only dropped to the level shown by nontargeted counterparts (Figure 4D). These findings point to the uptake capacity of DCs by pathways other than specific receptors, as expected on the basis of the results of nontargeted materials.

Previous studies revealed that Ag uptake by FcγR is not associated with endosomal or lysosomal compartments and was found colocalized with intracellular MHC class I,[55] thereby suggesting that FcγR-targeted Ag converge upon a class-I-processing pathway. In this regard, we studied the uptake of pH-sensitive FITC-labeled nanoformulations at various time points for a period of 24 h as indicated in Figure 4E. Fluorescence increased over this period of time, confirming that the endosomal/lysosomal pathway was overcome by the nanoparticles and liposomes.

(55) Guyre, C. A.; Barreda, M. E.; Swink, S. L.; Fanger, M. W. Colocalization of FcγRI-Targeted Antigen With Class I MHC: Implications for Antigen Processing. *J. Immunol.* **2001**, *166*, 2469–2478.

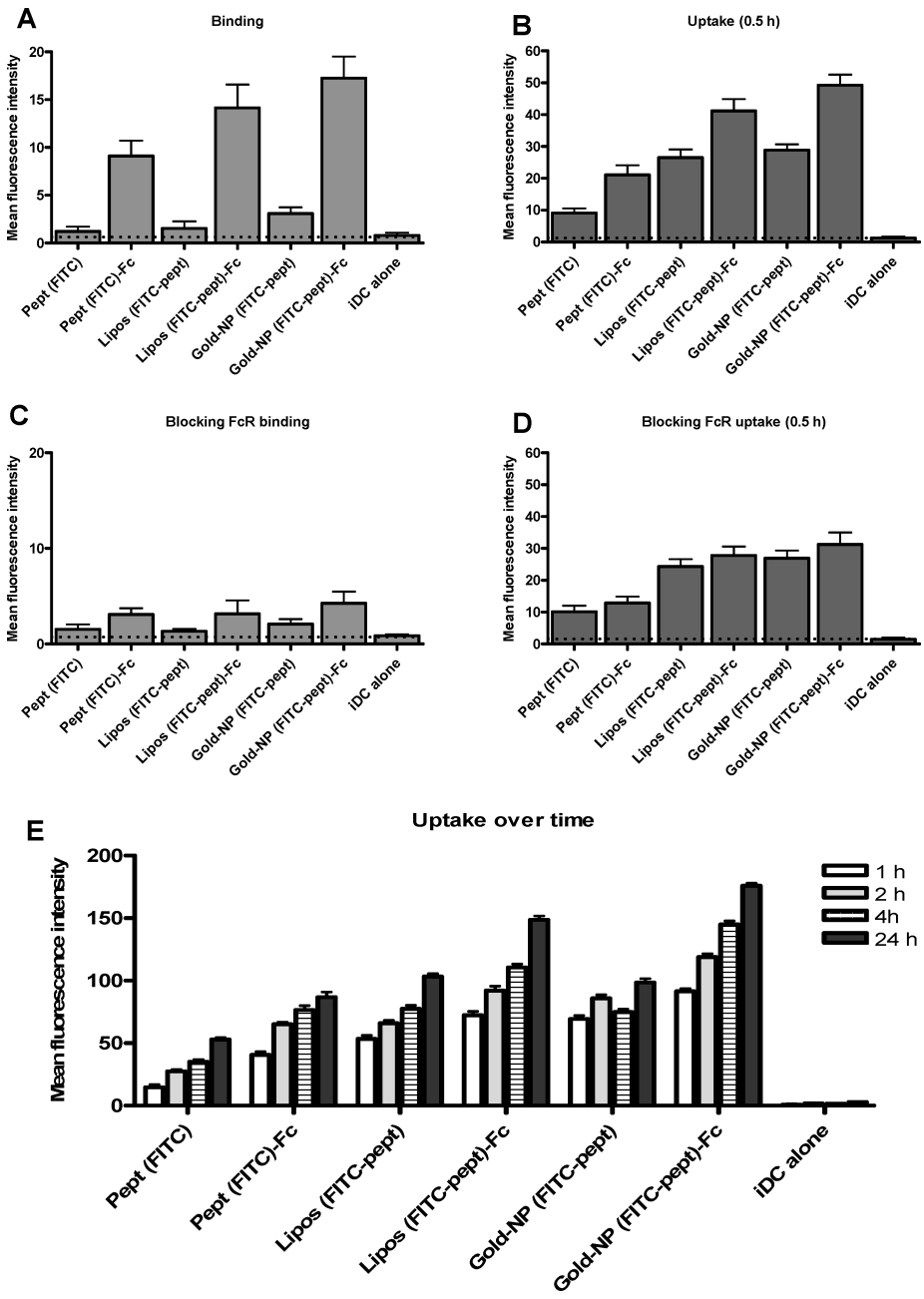

Figure 4. Flow cytometry analysis of binding and uptake of nanoparticles and liposomes. iDCs were collected, and free FITC-LHRH-TT peptide or peptide encapsulated in liposomes or nanoparticles (containing 10 μg/mL of FITC-peptide in each formulation), respectively, alone or with the Fc fraction of the human IgG (A). Peptides were then incubated with DCs previously cooled to 4 °C during 30 min to study binding without uptake. They were then washed in cold saline fixed and analyzed by flow cytometry (A). After the first acquisition, cells were incubated at 37 °C to determine Ag uptake and fluorescence measures were performed at 30 min (B), following the process previously described. In order to determine the contribution of the Fc-receptor interaction to binding and uptake, samples were pretreated in parallel for 30 min at 4 °C with or without an FcR-blocking reagent and then processed under the same conditions for binding (C) and uptake (D). Uptake kinetics was studied at 1, 2, 4, and 24 h as indicated above (E). The cells were then analyzed on a Coulter XL flow cytometer. Results are expressed in mean fluorescein intensity. Data are mean values ± SD of experiments performed in triplicate.

3.3. Internalization of Distinct Nanoformulations by CLSM. In order to study the influence of the Fc targeting on AuNP-conjugated and liposome-encapsulated peptides on the penetration and distribution of the Ag in DCs, fluoresced (FITC-peptide), unconjugated, conjugated, and encapsulated peptide was observed by CLSM. After incubation at 37 °C for a range of times, DCs were fixed with paraformaldehyde and examined under visible spectra light or excited at 488

nm with a laser beam for green fluorescence observation. Since differences in the fluorescence intensity were not as appreciable as by flow cytometry, only the pictures obtained at 4 h of incubation are presented in Figure 5.

CLSM confirmed the data obtained by flow cytometry, showing that all the preparations were taken up by DCs. However, differences were observed in the uptake of the nontargeted, targeted, and encapsulated peptides (Figure 5). In particular, we detected differences between the AuNP conjugates when they were targeted or not to FcRs. While all the conjugated and unconjugated Ag entered DCs, once inside their fate differed. In the AuNP conjugates, a diffuse labeling pattern was observed, while AuNPs targeted to FcRs showed a granulate pattern, suggesting their vacuole confinement. The distribution pattern of unconjugated peptides and liposome-encapsulated peptides did not appear to be diffuse and cytoplasm free, but was less defined. In the case of unconjugated peptides and liposome-encapsulated peptides, these patterns were less defined.

3.4. Localization Detected by TEM. Dual labeling of the AuNPs with fluorescence and gold allowed the study of the traffic in human DCs. Therefore, cellular localization of the AuNP conjugates was also studied by TEM. DCs were incubated for 60 min with either targeted or nontargeted AuNPs. Both kinds of conjugated AuNPs, those with and without the Fc fragment, were found dispersed in the cytoplasm; however, AuNP-peptide-Fc was often observed in specific compartments (Figure 6), thereby suggesting an active uptake by interaction with the FcR. There were no significant differences when the distinct kinds of AuNPs were incubated at different times before observation by TEM. This finding suggests rapid uptake by DCs (data not shown). The patterns observed by TEM were similar to those obtained from confocal microscopy (Figure 5), although fluorescence showed a more diffuse pattern. The differences in AuNP and AuNP-peptide uptake by DCs could be attributed to physicochemical changes in the net charge of the NPs induced by the incorporation of the peptide, which has a positive charge.

3.5. Induction of Autologous Lymphocyte Proliferation by in Vitro Immunization with the Distinct Formulations. DCs primed with the distinct nanoformulations at two peptide concentrations (2 and 10 μg/mL) were co-cultivated for 78 h with autologous lymphocytes at a 1/20 ratio (DCs/lymphocytes) in the presence of ^{3}H-thymidine for the last 18 h of culture. The radioactivity incorporated into DNA was studied as an indirect measure of lymphocyte proliferation. Unprimed DCs or DCs loaded with naked AuNPs were used as negative controls. SEB-primed DCs and PHA-stimulated lymphocytes were used as positive controls. Moreover, the acetyl-peptide and FITC-peptide were compared in order to demonstrate that the fluorescent label did not affect the Ag to be presented to Ag-specific T-cells (Figure 7).

AuNPs, liposomes, and peptide targeted to the FcR showed the greatest capacity to induce lymphocyte proliferation (Figure 7), with respect to peptide alone, nontargeted AuNP, and nontargeted liposomes.

In spite of the satisfactory results obtained with targeted peptide and liposomes, the AuNPs proved to be more efficient vehicles to transport Ag to DCs. In vitro immunization is a practical assay to perform a rapid test of immunological response; however, a number of factors must

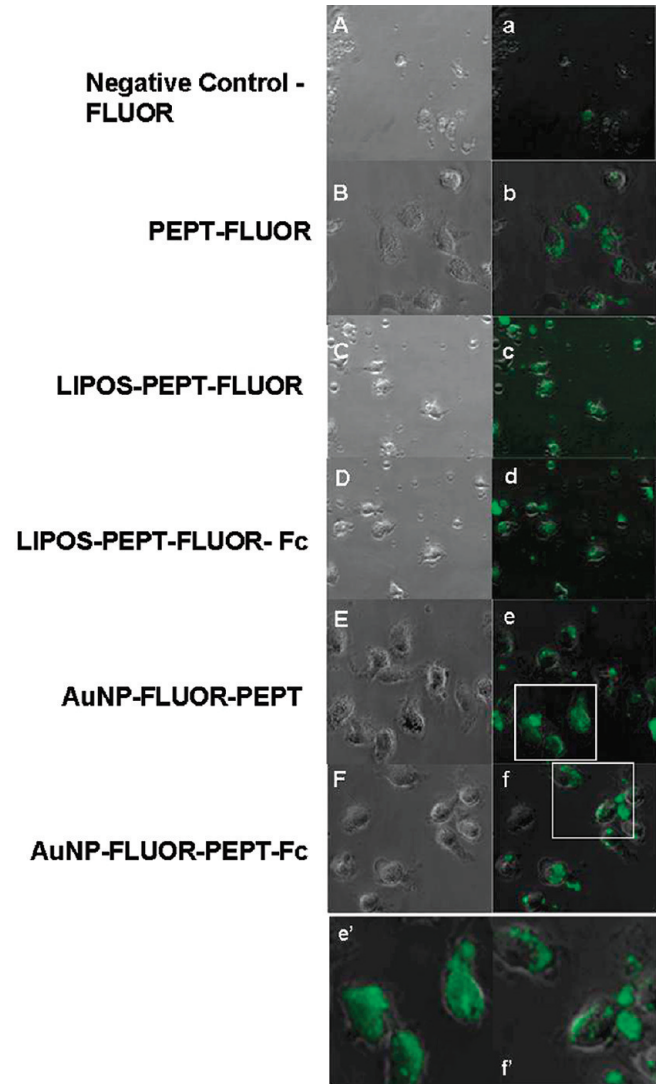

Figure 5. Confocal microspopy study in human DCs of naked peptides, peptides conjugated in AuNPs, and peptides encapsulated in liposomes. Images labeled in capital letters (left) are phase-contrast images of DCs incubated with the different formulations (except A-a, negative control), and images labeled with lower case letters (right) are a merge composition of the former with the fluorescent confocal images obtained concomitantly and synchronously. DCs cultured on slides were incubated at 37 °C for a range of times in order to study uptake. Only results at 4 h of incubation are shown. The pictures presented are the uptake of FITC-conjugated free LHRH-TT peptides (B), palmitoyl-peptide-FITC encapsulated in liposomes (C) or in liposomes targeted to Fc (D), and AuNPs with attached FITC-conjugated peptides alone (E) or with the Fc fraction of the human IgG (F). Untreated DCs (autofluorescence) were used as negative controls (A). Pictures (e′) and (f′) are magnifications of the white square inscribed in (e) and (f).

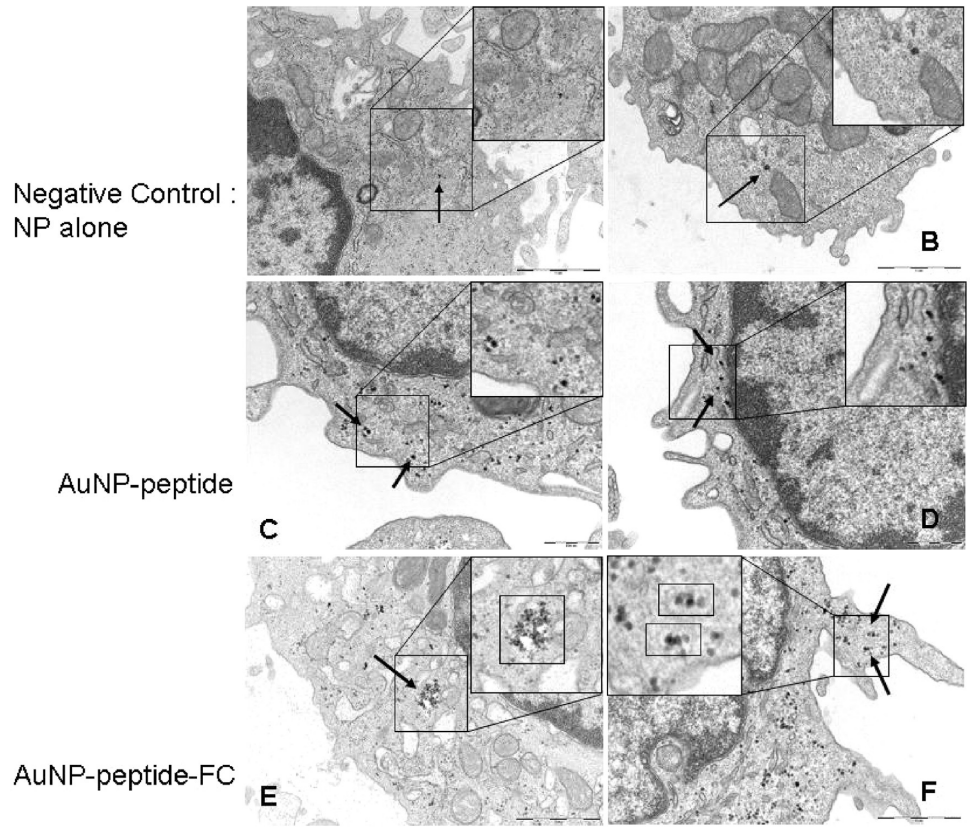

Figure 6. TEM images of the intracellular localization of AuNPs. iDCs incubated with the different preparations were fixed, and ultrathin sections were stained. Sections were then observed in a JEM-1010 electron microscope (JEOL, Japan). TEM images of human iDCs incubated with 13 nm naked NPs (A, B), nanoparticles complexed to peptide LHRH alone (C, D), or multiloaded with peptide LHRH and Fc (E, F). Some AuNPs complexed to peptide and Fc were located in cell vesicles. Regional magnifications of (C)−(F) are included as squares in the corner of the images.

be taken into account when evaluating the results. The Ag is concentrated in a well, and this does not reflect its biodistribution or dispersion by body fluids in in vivo models. Moreover, in the in vitro model, DC maturation (an essential step for an efficient immunological response) is induced by the addition of cytokines to the culture while adjuvants are required to stimulate this maturation in vivo. This would explain why the AuNPs targeted to the FcR is possibly the best selection, since the peptide is concentrated in the surface of the AuNPs and prevents Ag dispersion. This occurs because the AuNPs are directed to a receptor present on the surface of DCs, which, in addition, is specialized in the phagocytosis of pathological agents recognized by antibodies. Therefore, the activated DCs can mature and induce immune response (Figure 7).[26]

4. Conclusions

One of the greatest drawbacks for the development of vaccines for cancer immunotherapy is the low capacity of tumor Ag to induce an immune response strong enough to fight the tumor load and to overcome the frequent anergy present in cancer patients.

The peptide LHRH has been tested in animal models and humans and has been proven to induce specific antibodies.[40,56−65] In addition, this peptide shows T-cell activation capacity, as suggested by several algoritms, which predict peptide immunogenicity by epitope HLA binding.[66−70] However, the incorporation of a fragment of the tetanus toxoid makes a considerable contribution to increasing the

(56) Carelli, C.; Audibert, F.; Gaillard, J.; Chedid, L. Immunological castration of male mice by a totally synthetic vaccine administered in saline. *Proc. Natl. Acad. Sci. U.S.A.* **1982**, *79* (17), 5392–5395.
(57) Thau, R. Anti-LHRH and Anti-Pituitary Gonadotropin Vaccines: their Development and Clinical Applications. *Scand. J. Immunol.* **1992**, *36*, 127–130.
(58) Moudgal, N. R.; Jeyakumar, M.; Krishnamurthy, H. N.; Sridhar, S.; Krihsnamurthy, H.; Martin, F. Development of male contraceptive vaccine - a perspective. *Hum. Reprod. Update* **1997**, *3* (4), 335–346.
(59) Zhang, Y.; Rozell, T. G.; deAvila, D. M.; Bertrand, K. P.; Reeves, J. J. Development of recombinant ovalbumin-luteinizing hormone releasing hormone as a potential sterilization vaccine. *Vaccine* **1999**, *17* (17), 2185–2191.
(60) Ghosh, S.; Jackson, D. C. Antigenic and immunogenic properties of totally synthetic peptide-based anti-fertility vaccines. *Int. Immunol.* **1999**, *11*, 1103–1110.
(61) Sosa, J. M.; Zhang, Y.; de Avila, D. M.; Bertrand, K. P.; Reeves, J. J. Technical note: recombinant LHRH fusion protein suppresses estrus in heifers. *J. Anim. Sci.* **2000**, *78*, 1310–1312.
(62) Zeng, W.; Ghosh, S.; Lau, Y. F.; Brown, L. E.; Jackson, D. C. Highly immunogenic and totally synthetic lipopeptides as self-adjuvanting immunocontraceptive vaccines. *J. Immunol.* **2002**, *169* (9), 4905–4912.

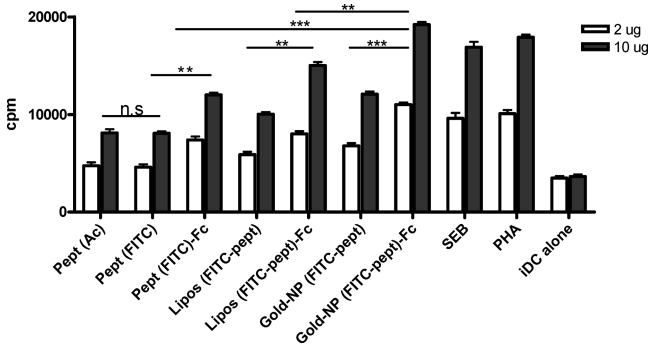

Figure 7. Analysis of lymphocyte proliferation induced by naked peptides, peptides conjugated with nanoparticles, and peptides encapsulated in liposomes. In vitro immunization was performed by incubation of the synthetic peptide formulations (naked peptides, peptide-AuNP,or peptide-liposomes with or without Fc (2 or 10 μg/mL of peptide)) on DC in culture until maturation. Next, autologous lymphocytes were added and co-cultured for 3 days (as described in Materials and Methods). The proliferation induced was measured indirectly by ^{3}H-thymidine incorporation during the last 18 h of culture. SEB was used as a positive control of DC-induced lymphocyte proliferation and PHA as a positive control of lymphocyte functionality. Results are expressed as directly counts per minute (cpm). Statistical significance is as follows: ** $p < 0.0$; *** $p < 0.001$. Data are mean cpm $\pm$ SD for four experiments.

induction of a T-cell response. Here we demonstrate that concentrating the peptide in liposomes or AuNPs is an efficient system to carry Ag to cells of the immunological system (mainly phagocytes such as DCs that act as Ag-presenting cells). Furthermore, targeting Ag to specific receptors present on DCs, which are specialized in the endocytosis of the Ag and DC activation, as is the case of Fcγ receptors, would prevent Ag dispersion in the bloodstream. Moreover, we have shown that this strategy not only increased Ag uptake with respect to the naked peptides but also almost doubled the lymphoproliferative response induced in these in vitro conditions, which are favorable to the Ag interaction with DCs, since Ag is continuously present in the assay well. This would not occur in an in vivo system, in which nontargeted Ag could be easily dispersed in the bloodstream.

The versatility of the system presented here allows the binding of several molecules, such as FITC, thereby allowing the tracking and monitoring of NPs by flow cytometry, CLSM, and TEM. Furthermore, in vitro immunization allows rapid and even high-throughput screening of distinct strategies for immunotherapeutic development.

In our conditions, the AuNPs targeted to the Fcγ receptor showed the best performance for Ag uptake and immunological response. This approach opens up the way to the development of an efficient system to design antitumor and other vaccines.

Abbreviations Used

AAA, amino acid analysis; C_{18}, octadecylsilica; DIEA, *N*,*N*-diisopropylethylamine; DMF, *N*,*N*-dimethylformamide; DCM, dichloromethane; DIPCDI, *N*,*N*′-diisopropylcarbodiimide; DBU, 1,8-diazabicyclo[5.4.0]-undec-7-ene; DHB, 2,5-dihydroxybenzoic acid; Fmoc, 9-fluorenylmethoxycarbonyl; HATU, 1-[bis-(dimethylamino)methylene]-1*H*-1,2,3-triazolo-[4,5-*b*]pyridinium-hexafluorophosphate 3-oxide; HOBt, 1-hydroxybenzotriazole; HOAt, 1-hydroxy-7-azabenzotriazole (3-hydroxy-3*H*-1,2,3-triazolo-[4,5-*b*]pyridine); HPLC, high pressure liquid chromatography; LHRH/GnRH, luteinizing hormone-releasing Hormone also known as gonadotropin-releasing hormone (GnRH); MALDI-TOF, matrix-assisted laser desorption ionization with time-of-flight analysis; MS, mass spectrometry; MSNT, 1-(mesitylene-2-sulfonyl)-3-nitro-1*H*-1,2,4-triazole; NMI, 1-methylimidazole; PyBOP, benzotriazol-1-yloxytris(pyrrolidino)phosphonium hexafluorophosphate; RP, reverse phase; TES, triethylsilane; TFA, trifluoroacetic acid; TBTU, 1-[bis(dimethylamino)methylene]-1H-benzotriazolium tetrafluoroborate 3-oxide; SMCC, sulfosuccinimidyl-4-(*N*-maleimidomethyl)cyclohexane-1-carboxylate; SPDP, *N*-succinimidyl-3-(2-pyridyldithio)-propionate.

Acknowledgment. This work was supported by a Grant from the "IV Convocatoria de Ayudas a la Investigación de la Fundación Mutua Madrileña". Also, this study was partially supported by ISCIII (CIBER-BBN 0074), the "Generalitat de Catalunya" (2005SGR 00662), the Institute for Research in Biomedicine, and the Barcelona Science Park.

MP100178K

(63) Jackson, D. C.; Lau, Y. F.; Le, T.; Suhrbier, A.; Deliyannis, G.; Cheers, C.; Smith, C.; Zeng, W.; Brown, L. E. A totally synthetic vaccine of generic structure that targets Toll-like receptor 2 on dendritic cells and promotes antibody or cytotoxic T cell responses. *Proc. Natl. Acad. Sci. U.S.A.* **2004**, *101* (43), 15440–15445.

(64) Finstad, C. L.; Wang, C. Y.; Kowalsky, J.; Zhang, M.; Li, M.; Li, X.; Xia, W.; Bosland, M. C.; Murthy, K. K.; Walfield, A. M.; Koff, W. C.; Zamb, T. J. Synthetic luteinizing hormone releasing hormone (LHRH) vaccine for effective androgen deprivation and its application to prostate cancer immunotherapy. *Vaccine* **2004**, *22*, 1300–1313.

(65) Zeng, W.; Gauci, S.; Ghosh, S.; Walker, J.; Jackson, D. C. Characterisation of the antibody response to a totally synthetic immunocontraceptive peptide vaccine based on LHRH. *Vaccine* **2005**, *23* (35), 4427.

(66) Rammensee, H. G.; Friede, T.; Stevanoviíc, S. MHC ligands and peptide motifs: 1st listing. *Immunogenetics* **1995**, *41* (4), 178–228.

(67) Rammensee, H. G.; Bachmann, J.; Emmerich, N. P. N.; Bachor, O. A.; Stevanovic, S. SYFPEITHI: database for MHC ligands and peptide motifs. *Immunogenetics* **1999**, *50*, 213–219; http://www.syfpeithi.de/Scripts/ MHCServer.dll/EpitopePrediction.htm.

(68) Parker, K. C.; Bednarek, M. A.; Coligan, J. E. Scheme for ranking potential HLA-A2 binding peptides based on independent binding of individual peptide side-chains. *J. Immunol.* **1994**, *152*, 163; http://www.bimas.cit.nih.gov/molbio/hla_bind/.

(69) Lundegaard, C.; Nielsen, M.; Lund, O. The validity of predicted T-cell epitopes. *Trends Biotechnol.* **2006**, *24*, 537–538.

(70) Lundegaard, C.; Lund, O.; Nielsen, M. Accurate approximation method for prediction of class I MHC affinities for peptides of length 8, 10 and 11 using prediction tools trained on 9mers. *Bioinformatics* **2008**, *24*, 1397–1398; http://tools.immuneepitope.org/analyze/cgi-in/mhc_I_ binding.py.